

TEMPORAL VARIATIONS OF SOLAR ROTATION DURING SOLAR CYCLE 23

Sarbani Basu¹ and H. M. Antia²

¹*Astronomy Department, Yale university, P.O. box 208101, New Haven CT 06520-8101, U. S. A.*

²*Tata Institute of Fundamental Research, Homi Bhabha Road, Mumbai 400005, India*

ABSTRACT

With 11 years of helioseismic data now available, we study the temporal variation in rotation rate in the solar interior. In addition to the well known zonal flow pattern, we also find that at low latitudes the pattern is shifting upwards with time and that the pattern extends almost to the base of the convection zone. By fitting a periodic function to the pattern it is possible to extract the temporal variation at each latitude and depth. This pattern can be compared with predictions of solar dynamo theories. We also examine possible periodic variations in the rotation rate in the tachocline region.

Key words: Sun: oscillations; Sun: rotation; Sun: interior.

1. INTRODUCTION

The solar rotation rate shows temporal variations. In the upper part of the convection zone bands of faster and slower than average rotating regions move towards the equator with time (Howe et al. 2000a; Antia & Basu 2000) at low latitudes, and towards the poles at high latitudes (Antia & Basu 2001). The low-latitude bands penetrate to the base of the convection zone and rise upwards with time (Basu & Antia 2003). Although early results (Howe et al. 2000a; Antia & Basu 2000) using limited data suggested that the zonal flow pattern penetrate to a depth of $0.1R_{\odot}$ only, later investigations find that the flows reach the base of the convection zone (Vorontsov et al. 2002; Basu & Antia 2003, 2006). This is in agreement with theoretical models of Covas et al. (2000) who also find the zonal flows penetrating through the convection zone.

The tachocline near the convection zone base is believed to be the seat of the solar dynamo, and changes may be expected in this region during the solar cycle. Howe et al. (2000b) have reported 1.3 yr oscillations in the rotation rate in equatorial region at $r = 0.72R_{\odot}$. However, this periodicity has not been seen in other works (e.g., Antia & Basu 2000; Corbard et al. 2001) and hence needs to be investigated further.

With the accumulation of GONG and MDI data over the last eleven years, it is possible to study the temporal variation in the rotation rate in the solar interior over a full solar cycle.

2. DATA AND TECHNIQUE

We use 105 temporally overlapping data sets from GONG (Hill et al. 1996) each covering a period of 108 days, starting from 1995 May 7 and ending on 2005 October 16, with a spacing of 36 days between consecutive data sets. The MDI data consists of 49 non-overlapping data sets each covering a period of 72 days, starting from 1996 May 1 and ending on 2006 May 20 (Schou 1999). Each set consists of the mean frequencies of different (n, ℓ) multiplets and the splitting coefficients. The GONG data includes up to 16 splitting coefficients, while MDI data has up to 36 coefficients.

We use 2D Regularised Least Squares (RLS) inversion technique (Antia et al. 1998) to infer the solar rotation rate for each data set. The time variation of rotation rate is obtained by subtracting the time-averaged rotation rate from the rotation rate at each epoch:

$$\delta\Omega(r, \theta, t) = \Omega(r, \theta, t) - \langle \Omega(r, \theta, t) \rangle, \quad (1)$$

where θ is the latitude and the angular brackets denote temporal average over the available data sets. The residual is the time-varying component of the rotation rate.

3. RESULTS

3.1. Zonal flows

Fig. 1 shows the cuts at constant radius for the temporally varying component of rotation velocity using GONG data. In the upper convection zone, the distinct bands of faster and slower than average rotation rate move towards the equator at low latitudes and towards the poles at high latitudes.

Fig. 2 shows the zonal flow pattern as a function of time and radius at a fixed latitude. We can see that the

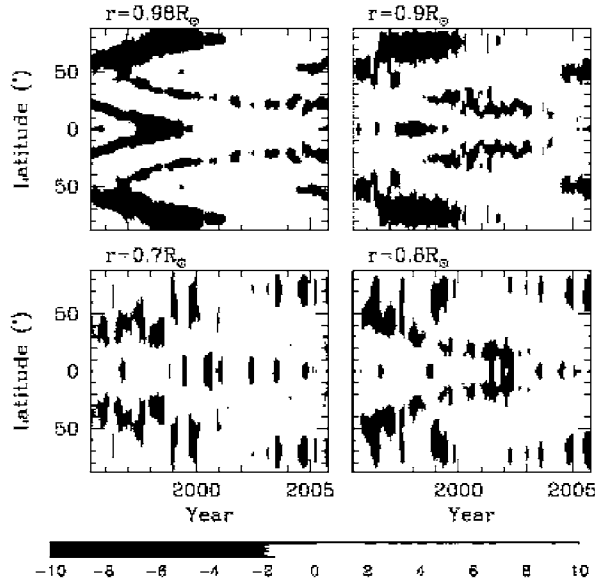


Figure 1. The rotation-velocity residuals (in m/s) at a few representative depths, obtained using 2D RLS inversion of GONG data. We have plotted $\delta v_\phi = \delta\Omega r \cos\theta$.

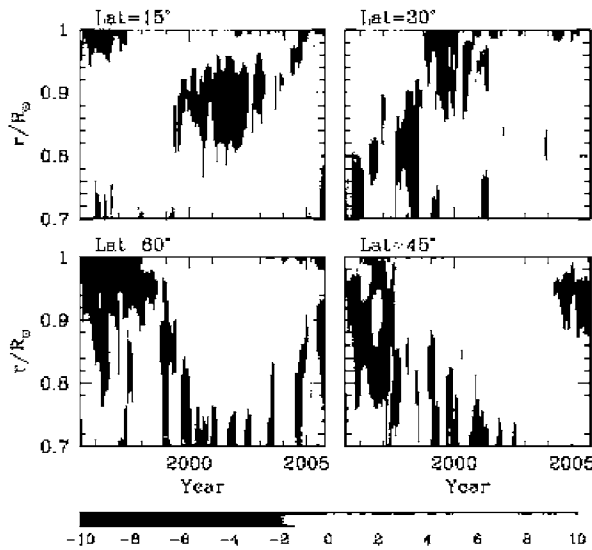


Figure 2. The rotation-velocity residuals (in m/s) as a function of time and radial distance at selected latitudes.

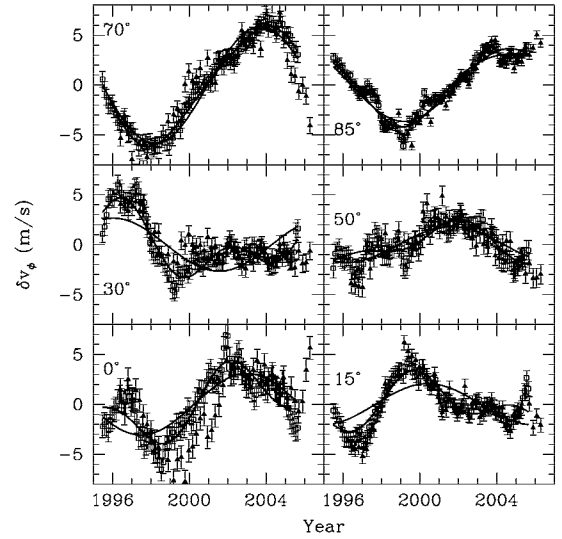


Figure 3. The zonal flow velocity as a function of time at different latitudes at $r = 0.98R_\odot$. The red and blue points show the results using GONG and MDI data while the lines show the fits to GONG data with period of 11 yr using Eq. 2 with only $k = 1$ term (green) and $k = 1, 2$ terms (cyan).

zonal flow pattern at 15° latitude penetrates to at least $r = 0.8R_\odot$, which is much deeper than earlier estimates (Howe et al. 2000a; Antia & Basu 2000). The pattern probably extends to the base of the convection zone (see also Vorontsov et al. 2002; Basu & Antia 2003, 2006). The fluctuations near the tachocline are most likely caused by data errors and hence, may not be significant. The bands seem to move upwards with time at a rate of about $0.05R_\odot$ per year i.e., about 1 m/s. The upward movement does not appear to be uniform. The zonal flow pattern appears to be similar at $r = 0.98R_\odot$ and $0.90R_\odot$, but is significantly shifted at deeper layers.

Fig. 3 shows the rotation velocity residuals at fixed radius and latitude plotted as a function of time. Different latitudes appear to be at different phases of the zonal-flow pattern. The magnitude of the flow is distinctly smaller around 50° than at other latitudes. This is also the latitude beyond which the shift in phase is less marked and gradual. If we assume that the zonal-flow pattern is periodic with a period of 11 years, the non-sinusoidal nature of variation in Fig. 3 implies the presence of higher harmonics of the period.

To the available data we can fit an expression of the form

$$\delta v_\phi(r, t, \theta) = \sum_{k=1}^N a_k(r, \theta) \sin(k\omega_0 t + \phi_k) \quad (2)$$

where, $\omega_0 = 2\pi/P_0$ is the basic solar cycle period, with $P_0 \approx 11$ years. The computed parameters a_k, ϕ_k can be used to predict the zonal flow pattern at any time. This fit also has the additional advantage of smoothing out the fluctuations in the data.

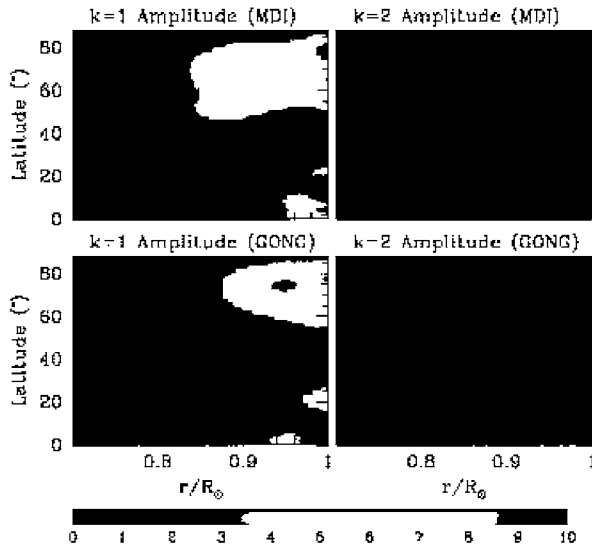


Figure 4. The amplitude (in m/s) of the $k = 1$ and 2 terms in the fit to zonal flow velocity.

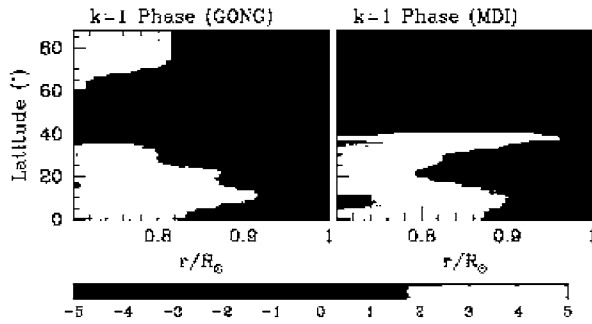


Figure 5. The phase (in radians) of the $k = 1$ term in the fit to zonal flow velocity. The phase is calculated with respect the surface value at the same latitude.

The amplitudes of the $k = 1$ and $k = 2$ components as a function of radial distance and latitude are shown in Fig. 4. It is clear that the first term dominates and the amplitude of higher harmonics is a small fraction of basic frequency (similar to results of Vorontsov et al. 2002 and Basu & Antia 2003). Higher-order terms other than $k = 2$ are not significant, a fact that was not very clear from earlier, limited data. Furthermore, from the amplitude of the $k = 1$ term it is clear that the pattern penetrates to a good fraction of the convection zone depth at low latitudes and possibly at high latitudes too. The highest amplitude is found in high latitude regions in the outer $0.1R_{\odot}$ layers. The pattern is not well defined at intermediate latitudes of around 40° as the amplitude in this region is rather small.

Fig. 5 shows the phase of $k = 1$ term. At each latitude the phase difference w.r.t. the surface value is shown. There is a rapid change in phase around $r = 0.85R_{\odot}$ at low latitudes, which is probably responsible for the change in pattern in deeper layers in Fig. 1. This change in phase may also have misled the early studies to conclude that the zonal flow pattern penetrates to a depth of

only $0.1R_{\odot}$. At high latitudes, the MDI data shows no significant variation in phase with depth, while GONG data shows some at very high latitudes in deeper layers, where the results may not be very reliable. Thus it appears that the high latitude part of the pattern is similar at all depths in the convection zone, though its amplitude reduces significantly with depth.

Using the parameters obtained by fitting Eq. 2 we can predict the zonal flow pattern at any time. Figs. 6 & 7 show the pattern obtained by fitting only the first two terms at some representative radius and latitudes over a period of 22 years. It is clear that the amplitude of zonal flows reduces with increasing depth. These can be compared with those from theoretical dynamo models. Because of fitting by Eq. (2) these patterns are smoother than those shown in Figs. 1 & 2.

3.2. The zonal flow and structure

It is known that the surface term obtained from asphericity inversions correlate well with the magnetic flux at the solar surface (Antia et al. 2001). Comparing zonal flows with the surface term (Fig. 8), we see that the surface term and the zonal flow pattern are well correlated and there is no evidence of a significant time lag between them. In order to see the relation between the zonal flow, the surface term in asphericity inversions and the surface magnetic field we fit a time profile given by Eq. (2) to each of these patterns at every latitude at the surface and the result is shown in Fig. 9. The magnetic field has been obtained from Kitt-Peak magnetograms. The phase has been chosen to make all curves continuous. It can be seen that if the phase of magnetic field at high latitudes is shifted upwards by 2π it will match that shown by the surface term in asphericity inversions. At intermediate latitudes where the amplitudes of all these patterns is low, the phase changes rapidly with latitude. In this region the behaviour of phase of magnetic field appears to be completely different, but this difference may not be significant as the amplitude of magnetic field in this region is very small and the fits may not have much significance. The amplitudes of all three patterns show a similar behaviour, with two prominent peaks in each hemisphere, one at low latitude and another at high latitude. The high latitude peak in surface magnetic field pattern is much lower than the low latitude peak.

3.3. The tachocline

To check for possible periodic oscillations near the tachocline region, we show $\delta\Omega$ at two radii in Fig. 10. This figure can be directly compared with Fig. 2 of Howe et al. (2000b). To test for periodicities in our results we calculate the discrete Fourier transform of $\delta\Omega$ and the results are shown in Fig. 9. It can be seen that none of the panels show any dominant peak. We do not see any significant periodic signal in either the GONG or the MDI results at these latitudes or depths.

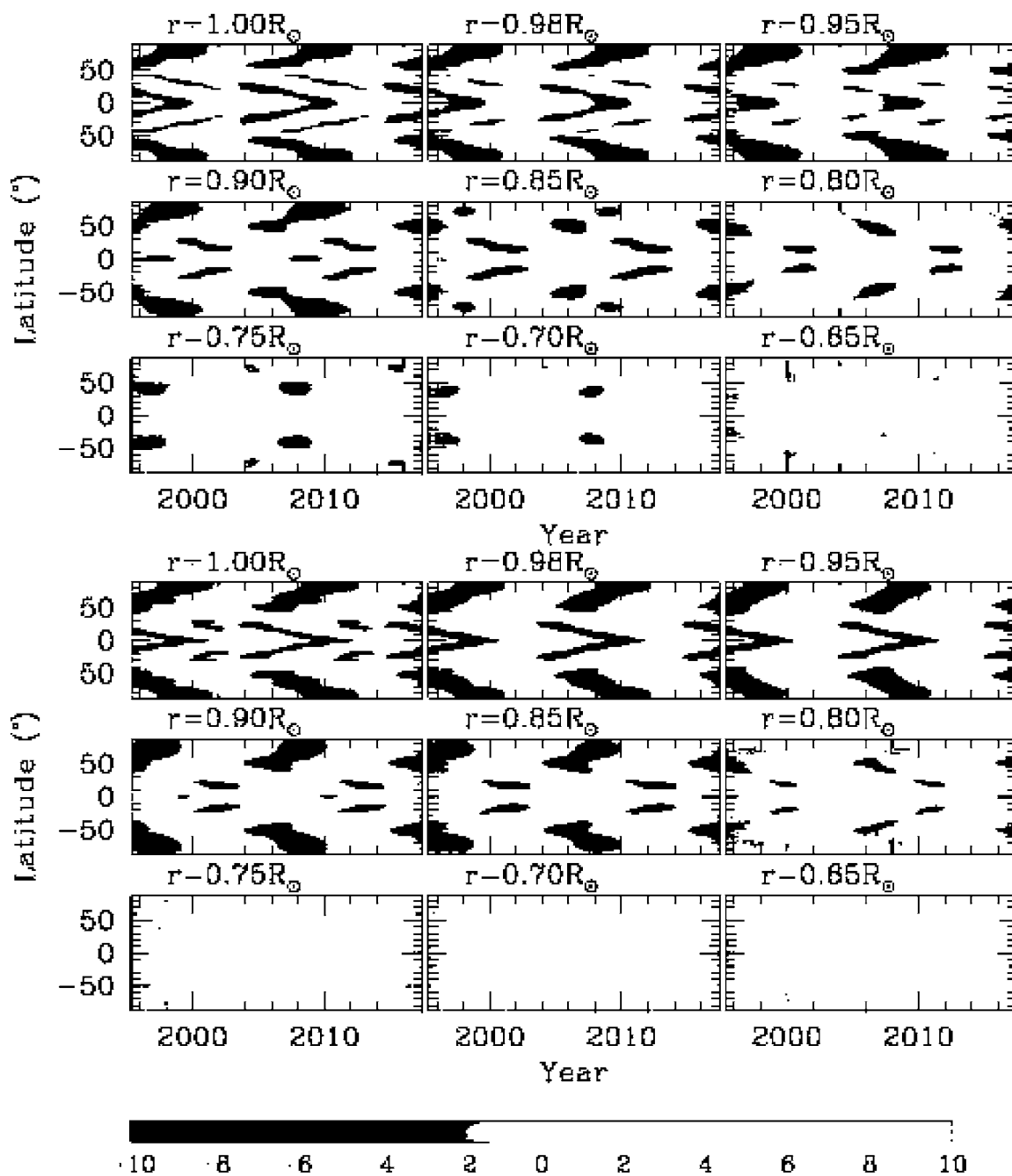


Figure 6. The predicted rotation-velocity residuals (in m/s) as a function of time and latitude at a few representative radius using the GONG (upper panels) and MDI (lower panels) data.

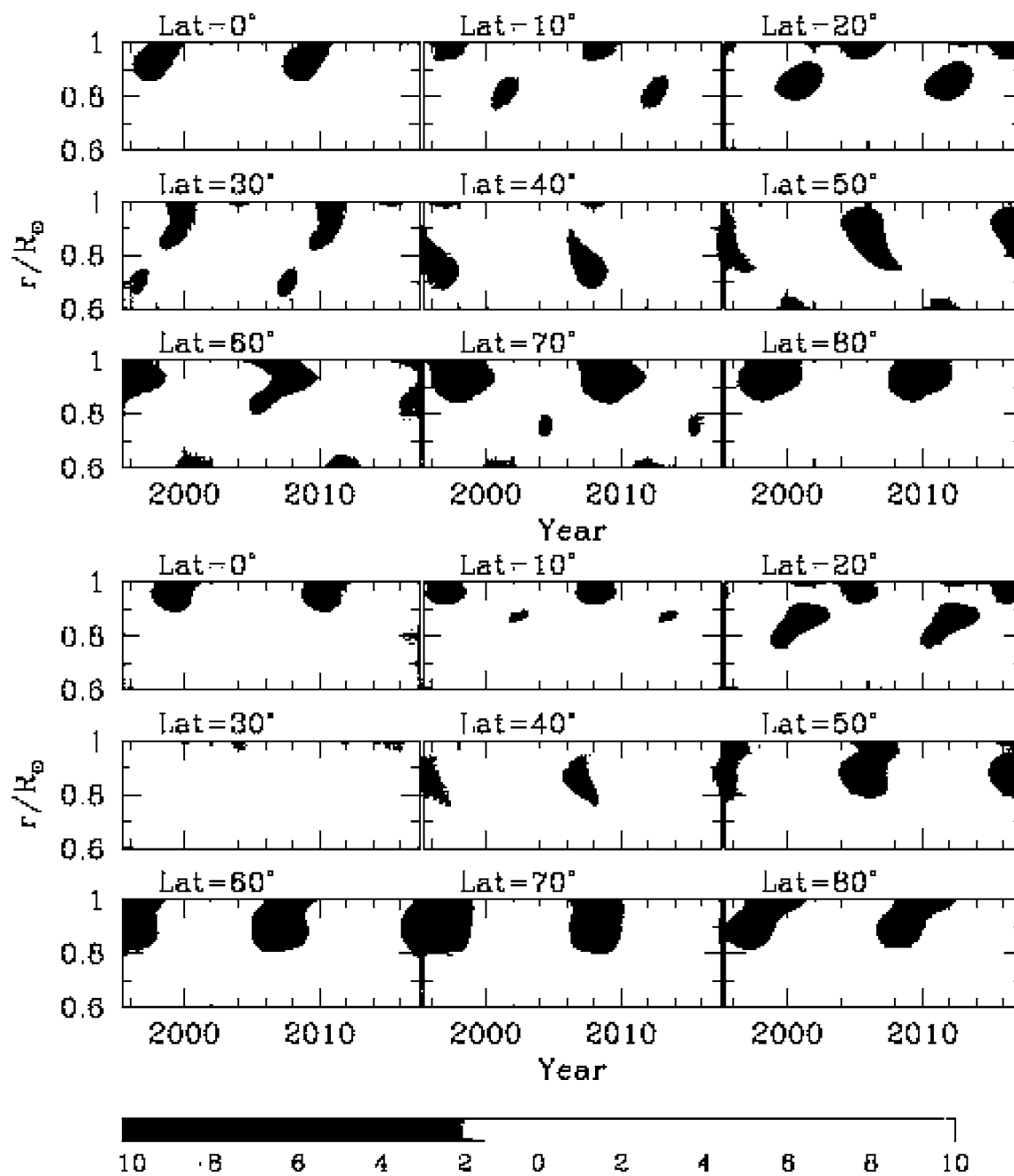


Figure 7. The predicted rotation-velocity residuals (in m/s) as a function of time and radius at a few representative latitudes using the GONG (upper panels) and MDI (lower panels) data.

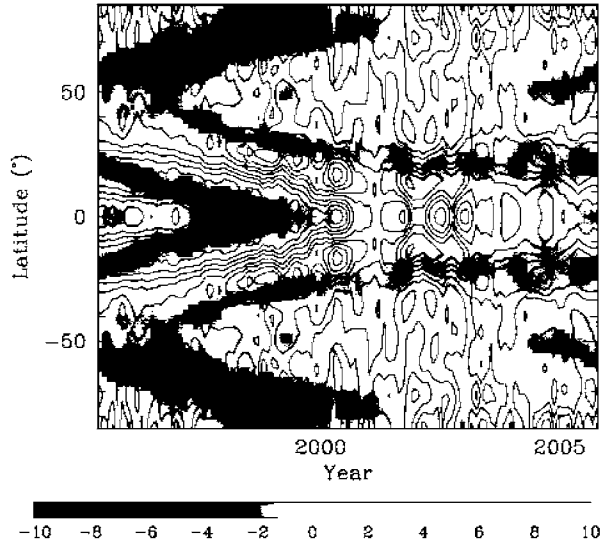


Figure 8. The contour diagram showing the surface term in asphericity inversions is superposed on the zonal flow pattern at $r = 0.98R_{\odot}$. The positive contours are shown by red lines, and negative ones by blue lines. The zonal flow is in units of m/s. The surface term is in arbitrary units.

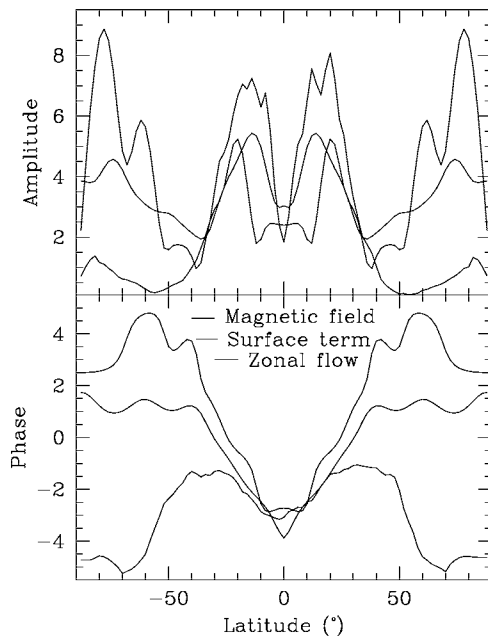


Figure 9. The amplitude and phase of zonal flow pattern, surface term in asphericity inversion and surface magnetic field. The amplitudes have been scaled to fit into the same figure.

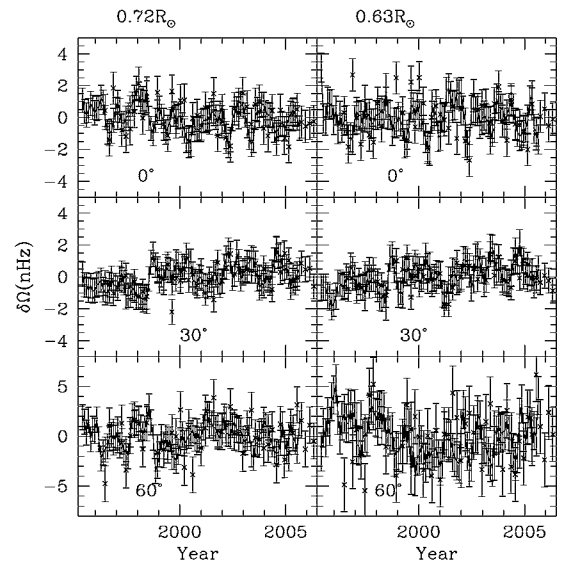


Figure 10. The rotation-rate residuals as a function of time at a few selected radii and latitudes. The radii are marked at the top of the figure, while latitudes are marked in each panel. 2D RLS inversion results from GONG are in red, MDI in blue.

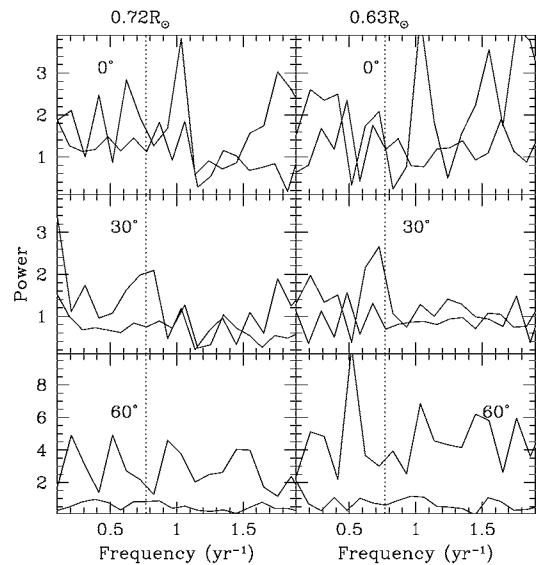


Figure 11. The discrete Fourier transform of the rotation-rate residuals at two radii (marked on top) and a few latitudes (as marked in each panel). GONG results are in red, MDI in blue. The dotted vertical line marks the 1.3 year period.

4. CONCLUSIONS

The rotation-rate residuals (obtained by subtracting the time-averaged rotation rate from that of each epoch) show the well known pattern of temporal variation that is similar to the torsional oscillations observed at the surface (Howard & LaBonte 1980). At low latitudes the bands move towards the equator with time. At high latitudes the bands appear to move towards the pole. This is quite similar to what is seen in theoretical results of Covas et al. (2000) based on a mean-field dynamo model. At low latitudes the bands of faster and slower rotation appear to move upwards at a rate of about 1 m/s. The zonal flow pattern penetrates almost to the base of the convection zone.

Assuming that the zonal flow pattern has a fundamental period of 11 years we find that in addition to the fundamental period, the second harmonic is also significant in outer layers. The phase at low latitude changes rapidly around $r = 0.85R_{\odot}$, while at high latitudes the phase doesn't show much variation inside the convection zone. The surface term from solar asphericity inversions correlates well with the zonal flow at the surface as well as with the surface magnetic field. At low latitudes the phases of these patterns are very similar, while at high latitudes there is some phase differences between the zonal flow and the surface term or surface magnetic field. The amplitude of all these three patterns also shows similar variation with latitude.

We do not find any evidence for the 1.3 year periodicity in equatorial regions at $r = 0.72R_{\odot}$, reported by Howe et al. (2000b).

ACKNOWLEDGMENTS: This work utilises data obtained by the Global Oscillation Network Group (GONG) project, managed by the NSO, which is operated by AURA, Inc. under a cooperative agreement with the National Science Foundation. The data were acquired by instruments operated by the Big Bear Solar Observatory, High Altitude Observatory, Learmonth Solar Observatory, Udaipur Solar Observatory, Instituto de Astrofísico de Canarias, and Cerro Tololo Inter-American Observatory. This work also utilises data from the Solar Oscillations Investigation / Michelson Doppler Imager (SOI/MDI) on the Solar and Heliospheric Observatory (SOHO). SOHO is a project of international cooperation between ESA and NASA. MDI is supported by NASA grant NAG5-8878 to Stanford University. This work is partially supported by NSF grant ATM 0348837 to SB.

REFERENCES

- Antia H. M., Basu S., 2000, ApJ 541, 442
 Antia H. M., Basu S., 2001, ApJ 559, L67
 Antia H. M., Basu S., Chitre S. M., 1998, MNRAS 298, 543
 Antia, H. M., Basu, S., Hill, F., Howe, R., Komm, R. W., & Schou, J. 2001, MNRAS 327, 1029
 Basu S., Antia H. M., 2003, ApJ 585, 553
 Basu S., Antia H. M., 2006, in Proc. SOHO17 '10 Years of SOHO and Beyond', ESA SP-617, eds. D. Spadaro, B. Fleck & J.B. Gurman, in press
 Corbard, T., Jiménez-Reyes, S. J., Tomczyk, S., Dikpati, M., Gilman, P., 2001, in Helio- and Astero-seismology at the Dawn of the Millennium, ed. A. Wilson (ESA SP-464; Noordwijk: ESA), 265
 Covas E., Tavakol R., Moss D., Tworkowski A., 2000, A&A 360, L21
 Hill F., et al., 1996, Science 272, 1292
 Howard R., LaBonte B. J. 1980, ApJ 239, L33
 Howe R., Christensen-Dalsgaard J., Hill F., Komm R. W., Larsen R. M., Schou J., Thompson M. J., Toomre J., 2000a, ApJ 533, L163
 Howe R., Christensen-Dalsgaard J., Hill F., Komm R. W., Larsen R. M., Schou J., Thompson M. J., Toomre J., 2000b, Science 287, 2456
 Schou J., 1999, ApJ 523, L181
 Vorontsov S. V., Christensen-Dalsgaard J., Schou J., Strakhov V. N., Thompson M. J., 2002, Science 296, 101